東北大学機関リポジトリ
TOUR
Tohoku University Repository

Improvements in quantum efficiency of excitonic emissions in ZnO epilayers by the elimination of point defects

著者	大友　明
journal or publication title	Journal of applied physics
volume	99
number	9
page range	093505-1-093505-6
year	2006
URL	http://hdl.handle.net/10097/40336

doi: 1063/1.2193162

Improvements in quantum efficiency of excitonic emissions in ZnO epilayers by the elimination of point defects

S. F. Chichibu,[a)] T. Onuma,[b)] M. Kubota, and A. Uedono[c)]
Institute of Applied Physics and Graduate School of Pure and Applied Sciences, University of Tsukuba, 1-1-1 Tennodai, Tsukuba 305-8573, Japan

T. Sota
Department of Electrical Engineering and Bioscience, Waseda University, Shinjuku 169-8555, Japan

A. Tsukazaki, A. Ohtomo, and M. Kawasaki[d)]
Institute for Materials Research, Tohoku University, Sendai 980-8577, Japan

(Received 10 August 2005; accepted 8 March 2006; published online 12 May 2006)

The internal quantum efficiency (η_{int}) of the near-band-edge (NBE) excitonic photoluminescence (PL) in ZnO epilayers was significantly improved by eliminating point defects, as well as by the use of ZnO high-temperature-annealed self-buffer layer (HITAB) on a $ScAlMgO_4$ substrate as epitaxial templates. Negatively charged Zn vacancy (V_{Zn}) concentration was greatly reduced by high-temperature growth, and slower postgrowth cooling (annealing) under minimum oxygen pressure further reduced the gross concentration of positively and negatively charged and neutral point defects, according to the suppression of nonequilibrium defect quenching. The nonradiative PL lifetime (τ_{nr}) at room temperature was increased by decreasing the gross concentration of point defects, as well as by decreasing the concentration of V_{Zn}. Accordingly, certain point defect complexes incorporated with V_{Zn} (V_{Zn}-X complexes) are assigned to the dominant nonradiative recombination centers. As a result of the elimination of point defects, a record long τ_{nr} (3.8 ns) at 300 K was demonstrated. Because the radiative lifetime (τ_r) is in principle constant in bulk and epitaxial ZnO, the increase in τ_{nr} gave rise to the increase in η_{int}. Rich structures originating from exciton-polaritons and excited states of excitons were eventually observed in the low-temperature PL spectrum of the improved ZnO epilayer on HITAB, of which η_{int} of the NBE emission was 6.3% at 300 K. © *2006 American Institute of Physics*. [DOI: 10.1063/1.2193162]

I. INTRODUCTION

ZnO and related (Mg,Zn,Cd)O alloys are an excellent candidate for the use in visible, ultraviolet (UV), and white light emitting diodes (LEDs) according to their large bandgap energies. Recently, a pending problem over the reproducible fabrication of *p*-type[1–3] ZnO has been solved by the radical nitrogen (N) doping using the repeated-temperature-modulation (RTM) method[4] during laser-assisted molecular-beam epitaxy (L-MBE). The sequence of RTM is the repetition of a 15 nm thick N-doped layer growth at 400 °C, subsequent rapid raising of the growth temperature (T_g) to 1050 °C, a 1 nm thick layer growth at 1050 °C, and rapid cooling of T_g to 400 °C. Stimulated with this achievment, Tsukazaki and most of the present authors[4] eventually observed UV and visible electroluminescence from ZnO *p-i-n* homojunction LEDs.

Prior to the *p*-type doping by RTM method instead of carrying out codoping or compensating the material, the growth of low residual electron concentration ZnO is quite essential, because the hole concentration is very low in N-doped[3,4] ZnO due to the large ionization energy of the N acceptor level (~100 meV) and poor substitution into the acceptor site. At the same time, the growth of low point defect concentration material is indispensable, because both structural and point defects are the sources of deep levels and nonradiative recombination centers (NRCs), which reduce the internal quantum efficiency (η_{int}) of the near-band-edge (NBE) emission. To accomplish the requirements, (i) a nearly lattice-matched $ScAlMgO_4$ (SCAM) substrate, of which in-plane lattice mismatch to ZnO is 0.09%, was selected[5] and (ii) a ZnO high-temperature-annealed self-buffer layer (HITAB) was introduced[6] for the L-MBE growth of ZnO. The concept of HITAB is to serve as a perfectly strain-free and atomically smooth, high crystallinity quasihomoepitaxial ZnO template for the overlayer growth. For this purpose, approximately 100 nm thick ZnO epilayer grown at 650–700 °C with 1×10^{-6} Torr of O_2 pressure (P_{O_2}) has been annealed at 1000 °C for 1 h in O_2 ambient. As a result of lattice relaxation and lateral mass transport by the high-temperature annealing, ZnO HITAB exhibiting a 0.26 nm high monolayer (ML) step-and-terrace surface structure with 10 μm wide terraces has been obtained.[6] By using HITAB on SCAM as the epitaxial template, atomically smooth ZnO

[a)]Author to whom correspondence should be addressed; also at NICP, ERATO, Japan Science and Technology Agency, Kawaguchi 332-0012, Japan and Photodynamics Research Center, RIKEN (Institute of Physical and Chemical Research), Aoba, Sendai 980-0868, Japan; electronic mail: optoelec@bk.tsukuba.ac.jp
[b)]Also at NICP, ERATO, Japan Science and Technology Agency, Kawaguchi 332-0012, Japan.
[c)]Also at Nanomaterials Laboratory, National Institute for Materials Science, Tsukuba 305-0003, Japan.
[d)]Also at Combinatorial Materials Exploration and Technology (COMET), Tsukuba 305-0044, Japan.

 © 2006 American Institute of Physics

Downloaded 09 Feb 2009 to 130.34.135.83. Redistribution subject to AIP license or copyright; see http://jap.aip.org/jap/copyright.jsp

epilayers exhibiting ML surface steps have been achieved. The values of full width at half maximum (FWHM) for the symmetric and asymmetric x-ray diffraction rocking curves of them were narrower than 18 sec. (instrumental resolution) and narrower than 30 sec., respectively.[4] However, photoluminescence (PL) lifetime (τ_{PL}) at room temperature of the NBE PL peak in the ZnO epilayer grown at $T_g=670$ °C on HITAB was as short as a few tenths of picosecond, which was even shorter than that of the ZnO epilayer grown directly on SCAM at 800 °C (110 ps).[7] These short τ_{PL} values indicate the presence of high density NRCs, because τ_{PL} at room temperature, especially in materials of low η_{int}, is generally dominated by the nonradiative lifetime (τ_{nr}) under the relations

$$\frac{1}{\tau_{PL}} = \frac{1}{\tau_r} + \frac{1}{\tau_{nr}} \tag{1}$$

and

$$\eta_{int} = \frac{1}{1 + \tau_r/\tau_{nr}}, \tag{2}$$

where τ_r is the radiative lifetime. Accordingly, the elimination of nonradiative and compensating point defects has been eagerly anticipated.

In order to develop an essential preparation method to decrease or even eliminate the NRCs, their atomic identity must be understood. For this purpose, the present authors[7,8] have correlated τ_{nr} and point defect species in ZnO epilayers grown directly on SCAM and ZnO substrates[7] by means of a combination of time-resolved photoluminescence (TRPL) and positron annihilation spectroscopy[9–12] (PAS) methods, according to the physical background that τ_{nr} can be obtained by TRPL measurement and PAS is the only method for detecting point defects in a condensed matter. Indeed, PAS is already an established technique for detecting negatively charged (or neutral) vacancy defects in semiconductors. The concept of PAS measurement is as follows. When a positron is implanted into condensed matter, it annihilates with an electron and emits two 511 keV γ rays. They are broadened due to the momentum component of the annihilating positron-electron pair. Because the momentum distribution of electrons in such defects is smaller than that in defect-free regions, they can be detected by measuring the Doppler broadening spectra of annihilation radiation. The change in the γ-ray spectra is characterized by S and W parameters;[8–12] the former mainly reflects the fraction of annihilating positron-electron pairs of small momentum distribution, and the latter represents the fraction of the pairs of large momentum distribution. Since Zn vacancies (V_{Zn}) and their complexes have negative charges forming acceptor-type defects in n-type ZnO,[8] they are the most probable candidates of positron trapping centers in ZnO. Therefore, S and W can be used as a measure of the concentration/size of V_{Zn}. For multilayer structures, characteristic S and positron diffusion length (L_+) in each layer can be determined by using a monoenergetic positron beam,[10] by which the mean implantation depth can be adjusted. The analysis[11] involves solving the diffusion equation of positrons using initial implantation profile as a function of positron acceleration energy E. The value of L_+ can be used as a measure of the gross concentration of positron trapping centers (V_{Zn} and V_{Zn} complexes) and scattering centers [positively charged and neutral point defects such as[13] oxygen vacancies (V_O), Zn interstitials (Zn_i), and complexes], because both decrease L_+.[7,8] Careful analysis on the $\tau_{PL}-S$ and $\tau_{PL}-L_+$ relations for the bulk[14,15] and epitaxial ZnO grown under various conditions[7] revealed that τ_{nr} increased with decreasing gross concentration of point defects and with decreasing concentration of V_{Zn} or V_{Zn} complexes. The results indicated that certain point defect complexes incorporated with V_{Zn} are the identity of NRCs.

In this article, the influence of point defect elimination on the static and dynamic responses of excitonic emissions are shown for L-MBE ZnO epilayers grown on ZnO HITAB on SCAM epitaxial templates, by means of temperature-dependent TRPL and PAS measurements. High T_g is found to be effective in reducing V_{Zn} concentration, and the postgrowth slow cooling (annealing) under minimum O_2 pressure significantly reduces the gross point defect concentration. As a result of overall process optimization, fine excitonic PL structures at low temperature and record long τ_{nr} (3.8 ns) at room temperature are demonstrated.

II. EXPERIMENT

The samples investigated were approximately 1 μm thick, undoped ZnO epilayers grown by combinatorial L-MBE.[4–6] A high-purity ZnO bulk single crystal grown by the seeded chemical vapor transport (CVT) method (Eagle-Picher Technologies, LLC) (Ref. 14) was ablated using the 248 nm line of a pulsed KrF excimer laser (5 Hz, 1 J/cm^2). The samples are categorized into five groups.

(I) ZnO on HITAB: Epitaxial growth of $(000\bar{1})$ ZnO was carried out between 800 and 1050 °C on ZnO HITAB templates, which were prepared by growing 100 nm thick ZnO at 650–700 °C ($P_{O_2}=1\times10^{-6}$ Torr) on (0001) SCAM substrates followed by *ex situ*[6] or *in situ*[4] thermal annealing at 1000 °C for 1 h in O_2 ambient. In order to study the effects of thermal history on $\tau_{PL}-S$ and $\tau_{PL}-L_+$ relations, postgrowth slow cooling was carried out on the epilayers grown on HITAB. The cooling rate (R_c) and P_{O_2} were varied in the ranges of −10 to −200 °C/min and 10^{-9}–10^{-3} Torr, respectively. For comparison, following samples[5,7,14,15] were also prepared.

(II) ZnO on SCAM: $(000\bar{1})$ ZnO epilayers were grown directly on SCAM substrates between 570 and 800 °C.[7] The growth orientation and T_g are abbreviated hereafter by $-c(x)$, where x is T_g without the unit (°C).

(III) ZnO on ZnO homoepitaxial films: Homoepitaxial $(000\bar{1})$ ZnO epilayers were grown at 550–670 °C on the bulk ZnO substrates prepared by the seeded CVT method.[14] The growth orientation and T_g are abbreviated by the same manner as (II).

(IV) a-plane ZnO on Al_2O_3: A nonpolar $(11\bar{2}0)$ a-plane ZnO epilayer was grown on $(10\bar{1}2)$ r-plane Al_2O_3 at

Downloaded 09 Feb 2009 to 130.34.135.83. Redistribution subject to AIP license or copyright; see http://jap.aip.org/jap/copyright.jsp

650 °C. The sample abbreviation is $a(650)/Al_2O_3$.

(V) bulk ZnO: A high-purity bulk ZnO single crystal grown by the seeded CVT method (Eagle-Picher Technologies, LLC) (Ref. 14) was also characterized. Its PL specterum at 8 K exhibited clearly split *A*- and *B*-excitonic polaritons and rich series of bound exciton lines.[15] All samples listed here exhibited a dominant NBE PL peak at 300 K, of which FWHM was 88–110 meV, depending on the film qualities.

High resolution steady-state PL spectra were measured using the 325.0 nm line of a cw He–Cd laser (6 W/cm^2) as the excitation source. PL was dispersed by a 67 cm focal-length grating monochromator, and phase-sensitive detection was carried out using a GaAs:Cs photomultiplier. The spectral resolution was 0.006 nm (nearly 70 μeV at a wavelength of 370 nm). TRPL measurements on the NBE PL peak were carried out using the 80 fs pulses of a frequency-doubled (2ω) mode-locked $Ti:Al_2O_3$ laser (361–363 nm, ~120 nJ/cm^2 per pulse) picked up at 8 MHz repetition rate. The TRPL signal was collected using a standard streak-camera acquisition technique.

A monoenergetic positron beam line[8] was used to measure the Doppler broadening spectra of annihilation radiation as a function of the incident positron energy *E*. For each value of *E*, a γ-ray spectrum with 5×10^5 total counts was measured. The low momentum part of the spectrum was characterized by the *S* parameter, which is defined as the number of annihilation events for the energy range of 511±0.76 keV. The high momentum part was characterized by the *W* parameter, which is calculated from the tail of the peak, where $3.4\ \text{keV} \leq |E-511\ \text{keV}| \leq 6.7\ \text{keV}$. The relationship between the *S* parameter and *E* was analyzed using the algorithm named VEPFIT, a computer program developed by van Veen *et al.*[11] The details of applying VEPFIT for multilayered structures are described elsewhere.[11] The one dimensional diffusion model of positrons is expressed by[9]

$$D_+\frac{d^2}{dz^2}n(z) - \kappa_{\text{eff}}(z)n(z) + P(z,E) = 0, \tag{3}$$

where D_+ is the diffusion coefficient of positrons, $n(z)$ is the probability density of positrons at a distance z from the surface, $\kappa_{\text{eff}}(z)$ is the effective escape rate of positrons from the diffusion process, and $P(z,E)$ is the implantation profile of positrons. The diffusion length of positrons $L_+(z)$ is given by

$$L_+(z) = \sqrt{D_+/\kappa_{\text{eff}}(z)}. \tag{4}$$

In the fitting procedure, the region probed by positrons was divided into two blocks, namely, the ZnO epilayer and the substrate. Under these conditions, VEPFIT was used to determine the fraction of positrons annihilated in each block and the corresponding *S* parameter. The *S*-*E* curve was fitted to the following equation:

$$S(E) = S_sF_s(E) + \sum S_iF_i(E), \tag{5}$$

where $F_s(E)$ is the fraction of positrons annihilated at the surface and $F_i(E)$ is the fraction of positrons annihilated in the *i*th block $[F_s(E)+\Sigma F_i(E)=1]$, and S_s and S_i are the *S* parameters of the surface and in the *i*th block, respectively.

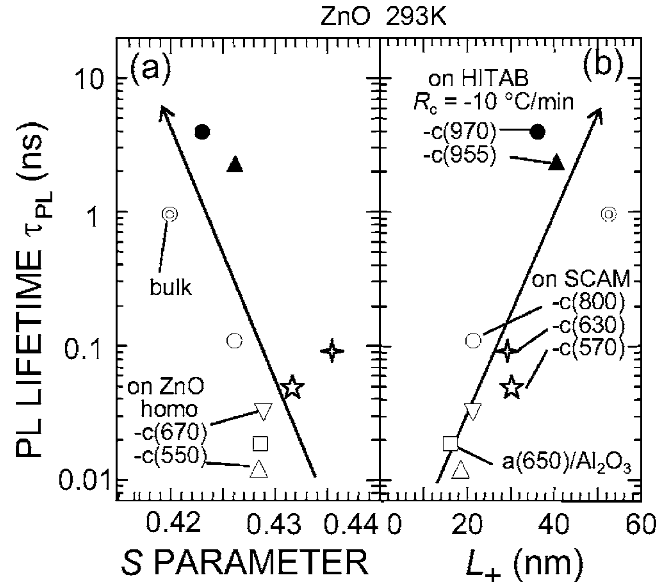

FIG. 1. PL lifetime (τ_{PL}) at 293 K for the near-band-edge (NBE) excitonic peak in ZnO epilayers as functions of (a) Doppler broadening *S* parameter of annihilation γ rays and (b) positron diffusion length L_+. For the samples of low internal quantum efficiency (η_{int}), τ_{PL} at room temperature is dominated by the nonradiative lifetime (τ_{nr}). Sample identification is written in the order of growth direction and T_g in bracket. Two samples plotted by closed characters were grown on ZnO high-temperature-annealed self-buffer layer (HITAB) prepared on SCAM substrates and cooled down slowly in near vacuum (R_c=−10 °C/min, P_{O_2}=10^{-9} Torr).

III. RESULTS AND DISCUSSION

The TRPL signal for the NBE excitonic PL peak in most of the samples exhibited biexponential but nearly single-exponential decay shape (data not shown).[7] The dominating τ_{PL} values at 293 K are plotted as functions of *S* and L_+ in Figs. 1(a) and 1(b), respectively. Note that the sample series (II), (III), and (IV) plotted by open characters were cooled down rapidly after the growth (–200 °C/min). Obviously, τ_{PL} increased with the decrease in *S* (reduction in V_{Zn}-related negatively charged point defect concentration) and with the increase in L_+ (reduction in gross concentration of positively charged, negatively charged, and neutral point defects); the results are similar to those obtained for GaN.[16] Because the correlativity for the τ_{PL}-L_+ relation is better than that for the τ_{PL}-*S* one, certain point defect complexes incorporated with V_{Zn}, namely, V_{Zn}-*X* complexes, are assigned to the identity of NRCs in ZnO. Note that single point defects in ZnO may not act as NRCs.[13]

In terms of the growth parameter, Fig. 1(a) gives a message that high T_g is preferable to obtain longer τ_{PL}, because *S* tended to decrease with the increase in T_g. However, there were exceptions such as ZnO on SCAM grown at 570 and 630 °C. Also, L_+ was often decreased as T_g was increased, as seen in the data for ZnO on SCAM in Fig. 1(b). These results suggest that high T_g gives rise to the reduction in V_{Zn} concentration but simultaneously gives rise to the increase in the concentration of positively charged or neutral point defects. Because most of the samples were cooled rapidly (R_c

Downloaded 09 Feb 2009 to 130.34.135.83. Redistribution subject to AIP license or copyright; see http://jap.aip.org/jap/copyright.jsp

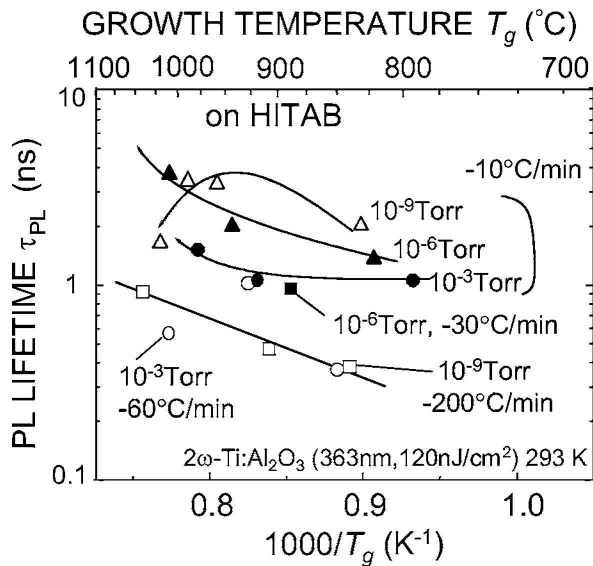

FIG. 2. (a) Value of $\tau_{PL}(\simeq\tau_{nr})$ at 293 K for the excitonic PL peak in ZnO epilayers grown on HITAB as functions of $1/T_g$ and postgrowth cooling conditions. Values of R_c and P_{O_2} are shown in the figure.

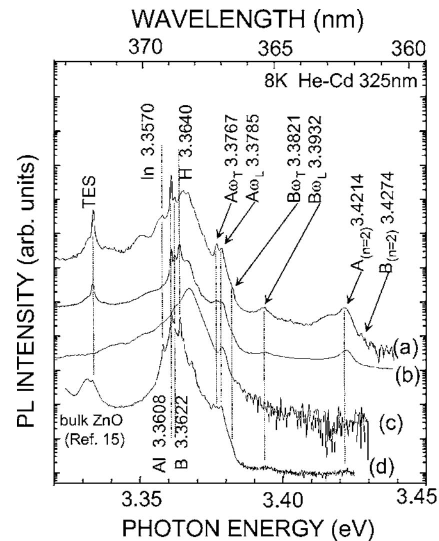

FIG. 3. PL spectra measured at 8 K of the ZnO epilayer grown on HITAB under the conditions (a) T_g=850 °C, R_c=−10 °C/min, $P_{O_2}=10^{-6}$ Torr, and (b) T_g=860 °C, R_c=−60 °C/min, $P_{O_2}=10^{-3}$ Torr. For comparison, PL spectra of the (c) ZnO epilayer grown directly on SCAM (T_g=800 °C) and (d) bulk ZnO single crystal grown by seeded CVT (Refs. 14 and 15) are also shown. Corresponding τ_{PL} at 293 K are 1.34 ns, 450 ps, 110 ps, and 970 ps for the samples shown in (a), (b), (c), and (d), respectively. Exciton-polariton structures became significant for the samples exhibiting longer τ_{PL}. PL peak energies are summarized in Table I.

=−200 °C/min) after the growth, unwanted quenching of nonequilibrium point defects such as V_O or Zn_i may be the cause of the decrease in L_+.

According to the hypothesis given above, postgrowth slow cooling was examined for the growth of ZnO on HITAB after high T_g growth. Values of τ_{PL} at 293 K for the ZnO epilayers prepared in this way are plotted as a function of $1/T_g$ in Fig. 2 for various R_c and P_{O_2} during cooling. As shown, τ_{PL} increased with the increase in T_g and with the decrease in $|R_c|$ and P_{O_2}. Although the surface of the sample grown at 1020 °C and cooled down in near vacuum (R_c =−10 °C/min, $P_{O_2}=10^{-9}$ Torr) was decomposed due to the sublimation, τ_{PL} reached 3.8 ns for the sample grown at 1020 °C and cooled in very low P_{O_2} ambient (R_c =−10 °C/min, $P_{O_2}=10^{-6}$ Torr). The results imply that for the samples grown at intermediate T_g up to 1000 °C, point defects can be decreased during the cooling in very low P_{O_2}. Therefore, it is reasonable to attribute the dominant positively charged defects that were annihilated during the cooling to Zn_i instead of V_O.[13] Consequently, the dominant NRCs in ZnO may involve V_{Zn}-Zn_i complex, presumably stabilized by the presence of H.[17] It should be noted that L_+ of the improved epilayers grown at high T_g on HITAB was increased to 40 nm or longer, as shown by closed characters in Fig. 1. By these means, a possiblity to improve η_{int} of the NBE emission is shown by (i) hardening the strain-free crystal lattice using HITAB on SCAM and (ii) carrying out appropriate defect management by high T_g growth and (iii) slower cooling under minimum P_{O_2}. As a matter of fact, high T_g was essential in realizing LEDs;[4] the undoped active layer and Ga-doped n-type layer were grown at 900–1000 °C and p-type conductivity was realized using RTM method, which involves the *lattice-hardening* procedure during very high-temperature 1 nm thick ZnO growth (similar to annealing).

High resolution PL spectrum at 8 K of the improved ZnO epilayer on HITAB (T_g=850 °C, R_c=−10 °C/min, $P_{O_2}=10^{-6}$ Torr) is shown in Fig. 3(a). As shown, rich structures due to excitons were observed, as is the case with the PL spectrum of a high-purity bulk ZnO single crystal grown by the seeded CVT method [see Fig. 3(d)].[15] The sample exhibited clearly split PL peaks between 3.376 and 3.394 eV, which originate from the lower and upper polariton branches (transverse and longitudinal excitons, respectively) of A and B excitons ($A\omega_T$, $A\omega_L$, $B\omega_T$, and $B\omega_L$). Also, PL peaks originating from the excited states of free A and B excitons [$A_{(n=2)}$ and $B_{(n=2)}$] and a band due to the excited states of bound excitons were observed at around 3.41–3.43 eV. Also, sharp PL lines due to the recombination of excitons bound to H, B, Al, In, and other impurities and defects[18] between 3.35 and 3.374 eV as well as the two-electron sattelites[3] (TES) at 3.3332 eV were clearly observed. Their peak energies and assignments are summarized in Table I. Note that the PL line at 3.3622 eV is assigned to the recombination of excitons bound to boron (B) donor, because the energy position seems to correspond to the energy for the group-III donor impurity shallower than Al.[19] Consequently, the line at 3.3640 eV is assigned to the volatile H donor, since its relative intensity decreased with increasing T_g.

These rich exciton features have never been reported for ZnO epilayers grown by any methods, indicating the excellent quality of the epilayer. Indeed, the optical quality of the epilayers was strongly influenced by the growth and cooling conditions even for those grown on HITAB. For example, PL spectra of ZnO epilayers grown under unoptimized preparation conditions are shown in Figs. 3(b) and 3(c). The sample shown in Fig. 3(b) was grown on HITAB with faster cooling in higher P_{O_2} ambient (T_g=860 °C, R_c=−60 °C/min, P_{O_2} $=10^{-3}$ Torr) and the sample shown in Fig. 3(c) was grown directly on SCAM at 800 °C with rapid cooling. As shown,

Downloaded 09 Feb 2009 to 130.34.135.83. Redistribution subject to AIP license or copyright; see http://jap.aip.org/jap/copyright.jsp

TABLE I. Near-band-edge PL peak energies at 8 K obtained for the ZnO epilayer grown on HITAB at 850 °C followed by the slow cooling (R_c=−10 °C/min, $P_{O_2}=10^{-6}$ Torr).

Energy (eV)	Label/origin	Reference (eV)
3.4274	$B_{(n=2)}$; $n=2$ B exciton	3.4290[a]
3.4214	$A_{(n=2)}$; $n=2$ A exciton	3.4231[a]
3.3932	$B\omega_L$; $n=1$ longitudinal B exciton	3.3941[a]
3.3821	$B\omega_T$; $n=1$ transverse B exciton	3.3830[a]
3.3785	$A\omega_L$; $n=1$ longitudinal A exciton	3.3783[a]
3.3767	$A\omega_T$; $n=1$ transverse A exciton	3.3768[a]
3.3740		
3.3722	I_0	3.3725[b]
3.3714	I_1	3.3718[b]
3.3702		
3.3689		
3.3667	I_3	3.3665[b]
3.3651		
3.3638	I_4; H	3.3628[b]
3.3622	I_5; B	
3.3608	I_6; Al	3.3608[b]
3.3600	I_8; Ga	3.3598[b]
3.3570	I_9; In	3.3567[b]
3.3557		
3.3510	(band)	
3.3332	TES	3. 333[c]
3.3321	(band)	

[a]Reference 15.
[b]Reference 3.
[c]Reference 18.

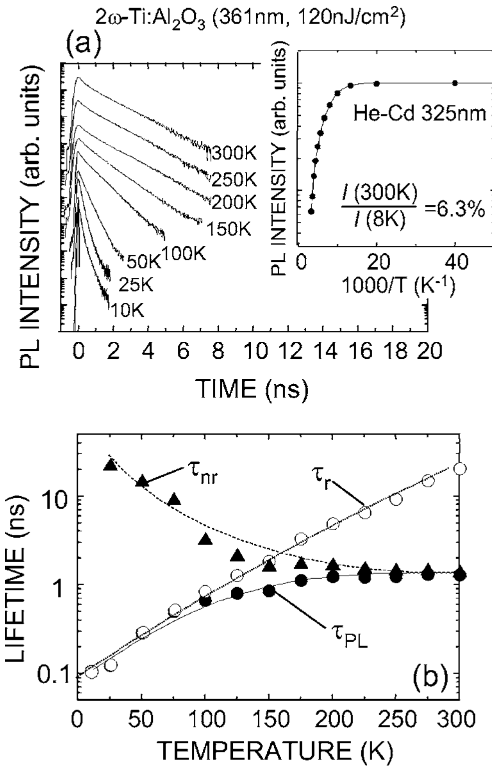

FIG. 4. (a) TRPL signals measured at the NBE PL peak energy for the ZnO epilayer grown on HITAB as a function of temperature (T). The sample was grown under the conditions T_g=850 °C, R_c=−10 °C/min, and $P_{O_2}=10^{-6}$ Torr. The inset shows the spectrally integrated NBE PL intensity as a function of $1/T$. At 300 K, η_{int} was 6.3%. (b) Values of τ_{PL}, τ_r, and τ_{nr} as a function of T. Values of τ_r and τ_{nr} were derived from τ_{PL} and η_{int} using Eqs. (1) and (2).

in comparison with the PL spectrum of the good sample [Fig. 3(a)], A-exciton polariton structures around 3.376–3.379 eV are not well resolved in Fig. 3(b), and overall exciton structures are degraded for Fig. 3(c). Note that the latter sample had a weak compressive strain, and A-exciton peak is shifted to the higher energy. The observed difference in the NBE PL spectra is attributed to the difference in the point defect concentration. Indeed, values of τ_{PL} at 293 K were 1.34 ns, 970 ps, 450 ps, and 110 ps for the samples shown in Figs. 3(a), 3(d), 3(b), and 3(c), respectively, and exciton structures degraded in this order.

The TRPL signal measured at the NBE peak energy for the improved ZnO on HITAB [the sample shown in Fig. 3(a)] is shown as a function of temperature (T) in Fig. 4(a). To visualize the improved η_{int}, which is substituted by the PL intensity at particular T divided by that at 8 K in this article, spectrally integrated normalized PL intensity is plotted as a function of $1/T$ in the inset. As shown, the TRPL signal exhibited a nearly single-exponential decay shape at all temperatures, and τ_{PL} increased with increasing T from 10 to 275 K [see Fig. 4(b)]. The result that η_{int} decreased but τ_{PL} increased with T indicates that τ_{PL} is dominated by τ_r up to relatively high temperatures. The values of τ_r and τ_{nr} were deduced from τ_{PL} and η_{int} using Eqs. (1) and (2) and are plotted in Fig. 4(b). Indeed, the critical temperature at which τ_r and τ_{nr} crossover was as high as 160 K, and thereby long τ_{nr} (1.31 ns) was obtaind at 300 K. As a result, η_{int} was as high as 6.3% at 300 K, which is approximately an order of magnitude higher than the typical value reported for low dislocation density GaN prepared by lateral epitaxial overgrowth techniques.[20] It should be noted that τ_r increased according to approximately $T^{1.5}$, which is characteristic of particles in three dimensional space.[21] The value of τ_r was 106 ps at 10 K and 20.6 ns at 300 K. The former value agrees with the one reported by Wilkinson *et al.*[22] for bound excitons in ZnO. The latter value seems reasonable for the net radiative lifetime of free excitons at 300 K, which may be limited by the free carrier lifetime. Consistently, τ_r at 300 K of the sample of intermediate quality [the sample shown in Fig. 3(b)] is also calculated to be 16 ns, from the values of η_{int} (2.8%) and τ_{PL} (450 ps).

IV. CONCLUSION

Reduction of the point defect concentration by the proper defect management is demonstrated as a fundamental pathway in obtaining semiconductor materials of high η_{int}. Results of TRPL and PAS measurements indicated that certain defect complexes involving V_{Zn} (V_{Zn}-X complexes) are the identity of NRCs in ZnO. Their concentration was decreased by increasing T_g and decreasing $|R_c|$ and P_{O_2} during cooling. The ZnO epilayer grown by L-MBE on HITAB over SCAM templates, of which η_{int} was 6.3% at 300 K, exhibited rich exciton-polariton features in its low-temperature PL spectrum. As a result of the overall process optimization, a long τ_{nr} at 300 K (3.8 ns) was obtained.

Downloaded 09 Feb 2009 to 130.34.135.83. Redistribution subject to AIP license or copyright; see http://jap.aip.org/jap/copyright.jsp

ACKNOWLEDGMENTS

This work was supported in part by the 21st Century COE program "Promotion of Creative Interdisciplinary Materials Science for Novel Functions" and Grant-in-Aid for Scientific Research Nos. 15656080, 16360146, and 14GS0204 by MEXT, Japan, the interuniversity cooperative program of IMR, Tohoku University, the Inamori Foundation, and AOARD (#04-4075)/AFOSR.

[1] K. Minegishi, Y. Koiwai, Y. Kikuchi, K. Yano, M. Kasuga, and A. Shimizu, Jpn. J. Appl. Phys., Part 2 **36**, L1453 (1997).
[2] M. Joseph, H. Tabata, and T. Kawai, Jpn. J. Appl. Phys., Part 2 **38**, L1205 (1999).
[3] D. C. Look, D. C. Reynolds, C. W. Litton, R. L. Jones, D. B. Eason, and G. Gantwell, Appl. Phys. Lett. **81**, 1830 (2002).
[4] A. Tsukazaki *et al.*, Nat. Mater. **4**, 42 (2005); A. Tsukazaki, M. Kubota, A. Ohtomo, T. Onuma, K. Ohtani, H. Ohno, S. F. Chichibu, and M. Kawasaki, Jpn. J. Appl. Phys., Part 2 **44**, L643 (2005).
[5] A. Ohtomo, K. Tamura, K. Saikusa, K. Takahashi, T. Makino, Y. Segawa, H. Koinuma, and M. Kawasaki, Appl. Phys. Lett. **75**, 2635 (1999); A. Ohtomo and A. Tsukazaki, Semicond. Sci. Technol. **20**, S1 (2005).
[6] A. Tsukazaki *et al.*, Appl. Phys. Lett. **83**, 2784 (2003).
[7] S. F. Chichibu *et al.*, Semicond. Sci. Technol. **20**, S67 (2005); T. Koida, S. F. Chichibu, A. Uedono, A. Tsukazaki, M. Kawasaki, T. Sota, Y. Segawa, and H. Koinuma, Appl. Phys. Lett. **82**, 532 (2003).
[8] A. Uedono, T. Koida, A. Tsukazaki, M. Kawasaki, Z. Q. Chen, S. F. Chichibu, and H. Koinuma, J. Appl. Phys. **93**, 2481 (2003).
[9] For a review, see, for example, R. Krause-Rehberg and H. S. Leipner, *Positron Annihilation in Semiconductors*, Springer Series in Solid-State Sciences 127, (Springer, Berlin, 1999).
[10] P. G. Coleman, *Positron Beams and Their Application* (World Scientific, Singapore, 2000), p. 1.
[11] A. van Veen, H. Schut, M. Clement, J. M. M. de Nijs, A. Kruseman, and M. R. Ijpma, Appl. Surf. Sci. **85**, 216 (1995).
[12] K. Saarinen *et al.*, Phys. Rev. Lett. **79**, 3030 (1997).
[13] A. F. Kohan, G. Ceder, D. Morgan, and C. G. Van de Walle, Phys. Rev. B **61**, 15019 (2000).
[14] D. C. Look, D. C. Reynolds, J. R. Sizelove, R. L. Jones, C. W. Litton, G. Cantwell, and W. C. Harsch, Solid State Commun. **105**, 399 (1999).
[15] S. F. Chichibu, T. Sota, G. Cantwell, D. B. Eason, and C. W. Litton, J. Appl. Phys. **93**, 756 (2003).
[16] S. F. Chichibu, A. Uedono, T. Onuma, T. Sota, B. A. Haskell, S. P. DenBaars, J. S. Speck, and S. Nakamura, Appl. Phys. Lett. **86**, 021914 (2005).
[17] E. V. Lavrov, J. Weber, F. Boerrnert, C. G. Van de Walle, and R. Helbig, Phys. Rev. B **66**, 165205 (2002).
[18] M. Strassburg *et al.*, Phys. Status Solidi B **241**, 607 (2004).
[19] B. K. Meyer, J. Sann, D. M. Hofmann, C. Neumann, and A. Zeuner, Semicond. Sci. Technol. **20**, S62 (2005).
[20] S. F. Chichibu *et al.*, Appl. Phys. Lett. **74**, 1460 (1999); A. A. Yamaguchi, Y. Mochizuki, and M. Mizuta, Jpn. J. Appl. Phys., Part 1 **39**, 2402 (2000).
[21] J. Feldmann, G. Peter, E. O. Göbel, P. Dawson, K. Moore, C. Foxon, and R. J. Elliot, Phys. Rev. Lett. **59**, 2337 (1987); H. Akiyama *et al.*, *ibid.* **72**, 924 (1994).
[22] J. Wilkinson, K. B. Ucer, and R. T. Williams, Radiat. Meas. **38**, 501 (2004).

Downloaded 09 Feb 2009 to 130.34.135.83. Redistribution subject to AIP license or copyright; see http://jap.aip.org/jap/copyright.jsp